Support Vector Regression to Accelerate Design and Crosspolar Optimization of Shaped-Beam Reflectarray Antennas for Space Applications

Daniel R. Prado, Jesús A. López-Fernández, Manuel Arrebola, *Senior Member, IEEE,* and George Goussetis, *Senior Member, IEEE*

***Abstract*—A machine learning technique is applied to the design and optimization of reflectarray antennas to considerably accelerate computing time without compromising accuracy. In particular, Support Vector Machines (SVMs), automatic learning structures that are able to deal with regression problems, are employed to obtain surrogate models of the reflectarray element to substitute the full-wave analysis tool for the characterization of the unit cell in the design and optimization algorithms. The analysis, design and optimization of a very large reflectarray antenna for Direct Broadcast Satellite applications are accelerated up to three orders of magnitude. This is here demonstrated with three examples: one showing the design of a reflectarray; and two for the crosspolar optimization, one with one coverage for each linear polarization (Europe and the Middle East) and another with a Middle East coverage working in dual-linear polarization. The accuracy of the proposed approach is validated by means of a comparison of the final designs with full-wave simulations based on local periodicity obtaining good agreement. The crosspolar dicrimination and crosspolar isolation are greatly improved using the SVMs while considerably reducing computing time.**

***Index Terms*—Machine learning techniques, Support Vector Machine (SVM), reflectarray, shaped beam antenna, Direct Broadcast Satellite (DBS), space communications**

I. Introduction

THE use of machine learning techniques to accelerate reflectarray analysis is a relatively recent research topic. The most widely used machine learning algorithms are Artificial Neural Networks (ANNs) [1]–[10], and more recently Kriging [11] and Support Vector Machines (SVMs) [12] are also being employed. These techniques can be used to obtain an efficient surrogate model using those algorithms to substitute the full-wave electromagnetic tool based on local periodicity (FW-LP) for the characterization of the unit cell. To that end, the FW-LP tool is employed to generate a number of samples of the electromagnetic behavior of the unit cell (i.e. the matrix of reflection coefficients) as a function of several input parameters (frequency, substrate, geometrical features, etc.). Those samples are used to train the ANN or SVM to obtain a function that matches the training samples and that is also able to predict the behavior of the unit cell for other values of the parameters which were not used in the training process.

In the past, ANNs have been employed to characterize the phase response of reflectarray unit cells [1]–[6]. This is useful since the phase response is the main parameter employed to carry out designs that meet given copolar requirements. Some works have been limited to a single polarization [1]–[4] while others characterized unit cells working in dual-linear polarization [5], [6]. More recently, ANNs have also been employed to predict the losses of the unit cell due to the substrate [7], [8] in addition to the phase-shift, and in other cases the cross-polarization [9] for dual-polarized unit cells. Kriging has also been employed to predict the phase response and losses [11], while SVMs have been used to characterize the whole matrix of reflection coefficients [12].

These algorithms substantially accelerate computations to carry out analysis of reflectarray antennas. In this regard, an application which goes one step further is to apply machine learning algorithms to the design of reflectarray antennas, where the analysis routine is called a hundreds or thousands of times in order to seek the unit cell geometry that provides the required phase-shift for each reflectarray element. For instance, in [10] ANNs are used along an optimization algorithm to find the optimum Minkowski cell and then to carry out a reflectarray design with a pencil beam pattern. In [6] a dual-linear shaped-beam reflectarray for Direct Broadcast Satellite (DBS) application is designed using ANNs achieving a speed-up factor of 207 with regard to a Method of Moments based on Local Periodicity (MoM-LP) [13].

The following natural step is to carry out optimization employing those algorithms in order to shape the radiation pattern using the geometrical features of the unit cell as optimizing variables. Until now, this has been accomplished using a MoM-LP tool directly in the optimization loop [14] or with databases [15], [16]. Although using the MoM-LP provides high accuracy for the computation of the reflection coefficient matrix, it penalizes the optimization with slow computations.

This work was supported in part by the European Space Agency (ESA) under contract ESTEC/AO/1-7064/12/NL/MH; by the Ministerio de Ciencia, Innovación y Universidades under projects TEC2017-86619-R (ARTEINE); by the Ministerio de Economía, Industria y Competitividad under project TEC2016-75103-C2-1-R (MYRADA); and by the Gobierno del Principado de Asturias through Programa "Clarín" de Ayudas Postdoctorales / Marie Courie-Cofund under project ACA17-09.

D. R. Prado and G. Goussetis are with the Institute of Sensors, Signals and Systems, School of Engineering and Physical Sciences, Heriot-Watt University, Edinburgh, U.K. (email: dr38@hw.ac.uk; G.Goussetis@hw.ac.uk).

J. A. López-Fernández and M. Arrebola are with the Department of Electrical Engineering, Group of Signal Theory and Communications Universidad de Oviedo, Gijón 33203, Spain (e-mail: jelofer@uniovi.es; arrebola@uniovi.es).

Color versions of one or more of the figures in this paper are available online at http://ieeexplore.ieee.org.

Digital Object Identifier XX.XXXX/TAP.XXXX.XXXXXXX

0000–0000/00$00.00 © XXXX IEEE

On the other hand, databases considerably accelerate computations using interpolation to predict the reflection coefficients. Another approach to accelerate computations is the use of machine learning algorithms such as ANNs or SVMs.

In this work, SVMs are used for the first time to carry out reflectarray design and optimization of copolar and crosspolar performances to substantially accelerate those processes with regard to the use of a FW-LP. In particular, the strategies developed in [12] are employed to train SVMs for the analysis of a large reflectarray for DBS application. The design process is detailed and carried out by a MoM-LP tool as well as the SVM to assess the accuracy and the computing time acceleration. Then, the same reflectarray is optimized to minimize the crosspolar pattern with MoM-LP and SVM, proving that machine learning algorithms are a promising technology to accelerate reflectarray analysis, design and optimization. Finally, the achieved acceleration for crosspolar optimization is discussed along with other techniques to further accelerate the crosspolar optimization of reflectarray antennas.

This paper is organized as follows. Section II provides a brief overview of the reflectarray analysis and SVM theory. Section III shows the results of using SVMs to the design of reflectarrays. In Section IV, SVMs are applied to the crosspolar optimization. Section V discusses the achieved acceleration with SVMs. Finally, Section VI contains the conclusions.

II. SVM Modeling of Reflectarray Unit Cell

Reflectarrays are classified as planar apertures and thus the radiation pattern may be efficiently computed from the tangential field applying the principle of equivalence [17]. The reflected tangential field at the reflectarray aperture is obtained from the incident field $\vec{E}_{\text{inc}}$ imposed by the feed as follows:

$$\vec{E}_{\text{ref}}(x_m, y_n) = \mathbf{R}^{mn} \vec{E}_{\text{inc}}(x_m, y_n), \tag{1}$$

where (x_m, y_n) are the coordinates of the (m, n)th reflectarray element and:

$$\mathbf{R}^{mn} = \begin{pmatrix} \rho_{xx}^{mn} & \rho_{xy}^{mn} \\ \rho_{yx}^{mn} & \rho_{yy}^{mn} \end{pmatrix}, \tag{2}$$

is the matrix of reflection coefficients and is obtained with a full-wave analysis based on local periodicity (FW-LP) [17]. ρ_{xx}^{mn} and ρ_{yy}^{mn} are known as the direct coefficients and mainly determine the shape of the copolar pattern through their phases for each polarization and the losses through their magnitude. On the other hand, ρ_{xy}^{mn} and ρ_{yx}^{mn} are the cross-coefficients and contribute significantly to the crosspolar pattern. Thus, a correct prediction of both copolar and crosspolar patterns requires the full characterization of (2).

Once the tangential reflected field in (1) has been obtained, the far field is efficiently computed using the Fast Fourier Transform (FFT) and applying the first principle of equivalence [14]. Finally, the copolar and crosspolar components are obtained using Ludwig's third definition of crosspolarization [18].

Since the far field is efficiently computed using the FFT, the most time consuming operation in the reflectarray analysis is the computation of (2) using a FW-LP for each reflectarray element. The goal of the SVMs is to obtain a surrogate model of each reflection coefficient which is able to predict the electromagnetic behavior of the unit cell as a function of certain parameters.

A. Surrogate Model Based on SVM

SVMs are automatic and supervised learning algorithms which are used to solve regression and classification problems [19]. For the purposes of this work, the regression features of the SVMs are adapted to find a surrogate model of the reflectarray unit cell. Here we will merely review the basic concepts necessary to understand the approach that follows and refer the reader to [12] for details.

SVMs use a training set comprised of a series of inputs and outputs, $T = \{\vec{x}_i, y_i\}_{i=1,\,2,\,\ldots,\,N_r}$ with $\vec{x}_i \in \chi \subseteq \mathbb{R}^L$ and $y_i \in \mathbb{R}$, to obtain a function f that estimates the output $(\widetilde{y})$ corresponding to any new input $\vec{x} \in \chi$. The function f takes the form:

$$f(\vec{x}) = \widetilde{y} = b + \sum_{i=1}^{N_s} \left[\left(\alpha_i^- - \alpha_i^+ \right) K(\vec{x}_i, \vec{x}) \right], \tag{3}$$

where b is the offset; N_s is the number of support vectors; α_i^- and α_i^+ are the optimal Lagrange multipliers; $\vec{x}_i$ are the support vectors, and $K(\cdot\,,\cdot)$ is the kernel function. In this work, we use a Gaussian Kernel that follows the equation:

$$K(\vec{x}, \vec{x}\,') = \exp\left(-\gamma \left\| \vec{x} - \vec{x}\,' \right\|^2\right), \tag{4}$$

where γ is a tunable parameter [12] and $\| \cdot \|$ stands for the Euclidean norm.

The function f of the SVM model minimizes a regularized risk functional that accounts for the empirical errors (weighted by parameter C) and for the flatness of f. In addition, we use the ϵ-insensitive loss function to compute the empirical errors. The parameters C, ϵ and γ determine the shape of the regression function f and they must be selected carefully to achieve an accurate estimation of new outputs. In particular, the SVM training was carried out considering 1750 samples for the training set, 375 samples for the validation set and 375 samples for the test set. The parameter ϵ is dynamically calculated as a function of the desired error and output samples, while C and γ are found following the efficient grid search detailed in [12].

The considered reflectarray unit cell is depicted in Fig. 1. It is comprised of two layers of dielectric substrate having two sets of parallel and coplanar dipoles shifted half a period with respect to each other. Each set of four parallel dipoles controls the phase-shift of a linear polarization. The SVM is trained to estimate the reflection coefficient matrix in (2) starting from a training set of samples that, in this work, is obtained using the MoM-LP described in [20].

All the parameters on which matrix $\mathbf{R}^{mn}$ depends on may be taken as input variables of the SVM training. Nonetheless, in order to reduce the complexity of the training process and to further improve the accuracy of the surrogate model, we reduce the number of input variables and set some of them to fixed values. The working frequency is set to 11.85 GHz and the periodicity to 14 mm$\times$14 mm. The selected substrate

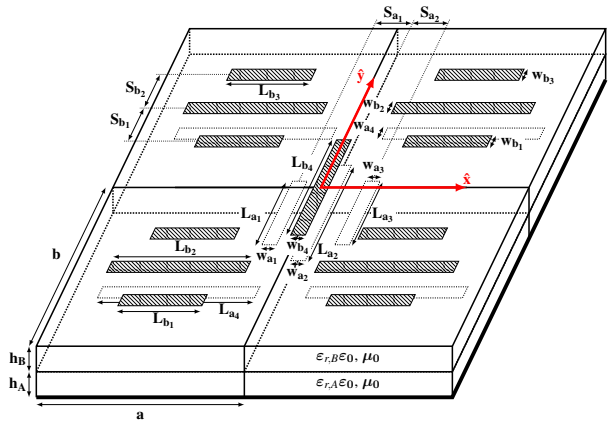

(a)

Fig. 1. Reflectarray unit cell consisting of two layers of parallel and coplanar dipoles divided in two sets of four dipoles per linear polarization.

has a height of 2.363 mm and a complex relative permittivity $\epsilon_r = 2.55 - j2.295 \cdot 10^{-3}$ for the bottom layer, while the top layer has a height of 1.524 mm and a complex relative permittivity $\epsilon_r = 2.17 - j1.953 \cdot 10^{-3}$. In addition, only the length of the dipoles will be used as training variables, thus fixing the width of the dipoles to 0.5 mm and the separation between them to 4 mm. This leaves eight geometrical variables to train the SVMs plus two angles of incidence. Following the strategy in [12], the geometrical variables are reduced to two, T_x and T_y, with the lengths of the dipoles proportional to those variables according to the following relations [21]:

$$\begin{aligned} &L_{a_4} = T_x \;\; ; \;\; L_{b_1} = L_{b_3} = 0.63\,T_x \;\; ; \;\; L_{b_2} = 0.93\,T_x, \\ &L_{b_4} = 0.95\,T_y \;\; ; \;\; L_{a_1} = L_{a_3} = 0.58\,T_y \;\; ; \;\; L_{a_2} = T_y. \end{aligned} \tag{5}$$

These relations were found by other authors using MoM-LP, seeking a linear phase response and a broadband performance. In addition, one SVM will be trained per angle of incidence.

Since the SVMs are conceived to estimate real-valued functions and the reflection coefficients are complex numbers, we need at least eight SVM models to characterize (2). In this work, for each incident angle, we obtain one SVM model for the real part of each reflection coefficient, another for the imaginary part, plus two additional models to estimate the magnitude of the direct coefficients. This makes a total of ten SVM models per angle of incidence. In addition, using the proposed smart grid search in [12] to find the optimum C, ϵ and γ parameters, the mean training time per SVM is 63 seconds; this is approximately three orders of magnitude lower than an exhaustive grid search, achieving a similar error.

Fig. 2 shows the results comparing the surrogate model of ρ_{xx} and ρ_{xy} with the MoM-LP simulation for an oblique incidence of $(\theta = 29°,\ \varphi = 55°)$. The agreement between the SVM model and MoM-LP is excellent for the direct coefficient in both magnitude and phase, and in the magnitude of the cross-coefficient; while there are slight discrepancies in the phase of ρ_{xy} due to its highly variability. Overall, the agreement is very good and the differences are mainly produced at those points where the phase of the cross-coefficient abruptly changes. This accuracy is expected to be the same as direct

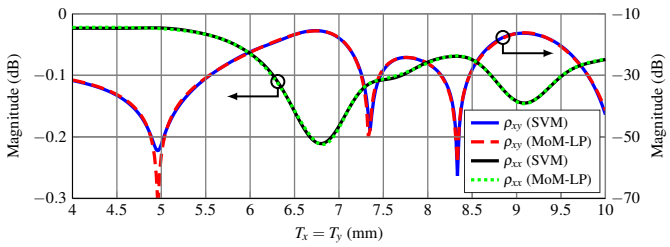

(a)

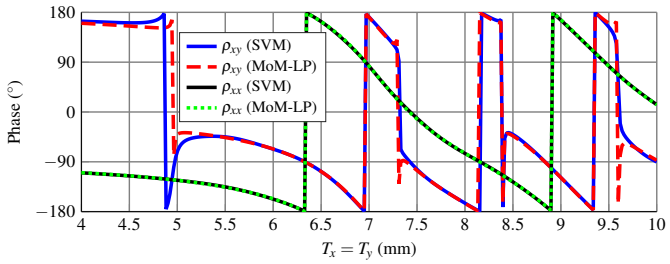

(b)

Fig. 2. Comparison of ρ_{xx} and ρ_{xy} for $(\theta = 29°,\ \varphi = 55°)$ between SVM and MoM-LP as a function of T_x and T_y for the cut $T_x = T_y$ in (a) magnitude in dB and (b) phase in degrees.

interpolation in databases using high-order splines.

Finally, we have opted for a 2D problem to achieve a highly accurate SVM model. In light of the results of other works in the literature [5], [22] dealing with machine learning algorithms in higher dimensions, it may be possible the use of SVMs to increase the number of available degrees of freedom for reflectarray optimization. Nevertheless, as it will be shown in Section IV, the improvement of the achieved results with two variables per element is significant with regard to the starting point.

III. Accelerating Reflectarray Design with SVMs

A. Design Procedure

The design procedure of a reflectarray antenna consists of finding, for each reflectarray element, the dimensions of the element which produces the desired phase-shift. The required phase-shift may be obtained analytically for canonical patterns such as pencil beams or more generally by means of a Phase-Only Synthesis (POS) for shaped-beams [17]. If the reflectarray works in one polarization, only one phase-shift distribution will be obtained. On the other hand, for dual-polarized reflectarrays, two phase-shifts per element are required, and both need to be matched by the geometry of the unit cell depending on the polarization of the impinging wave coming from the feed. Here, we will detail the design procedure aimed at obtaining the layout of dual-linear polarized reflectarrays.

The design procedure followed in this work is illustrated in Fig. 3. First, a table of phase-shifts is generated varying T_x and T_y in little steps. The phase-shift obtained modifying each variable is practically uncoupled [23], so this is done independently for each polarization. In this way, we select two values for each variable T_x and T_y which provide a phase-shift that is close to the required one, but a little above and below the exact value. Then, using a linear equation, the approximate

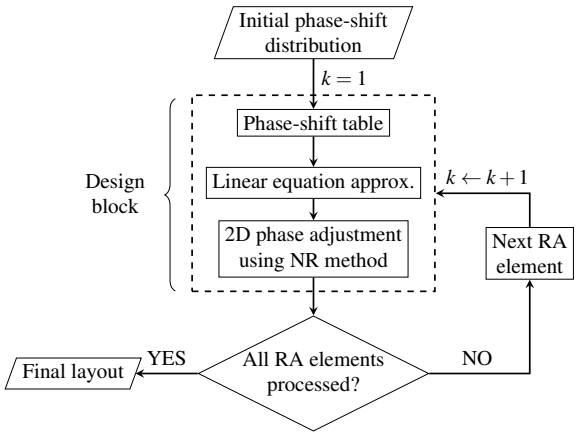

Fig. 3. Flowchart of the design procedure from the required phase-shift to the final reflectarray layout.

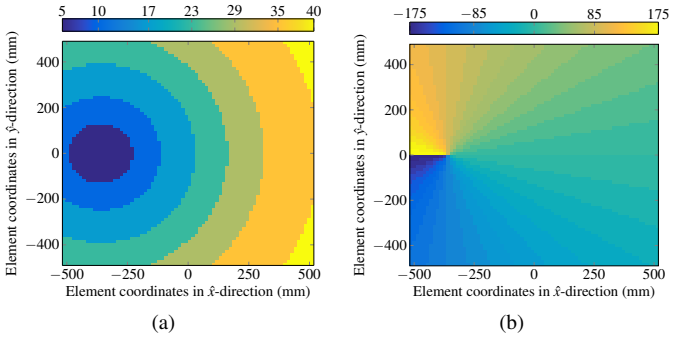

Fig. 4. Discretization of the angles of incidence. (a) θ. (b) φ.

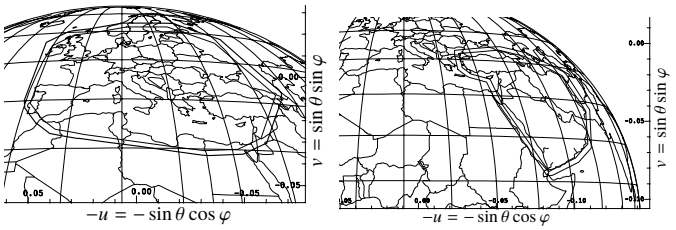

Fig. 5. Coverages for DBS application with (u, v) coordinates in the antenna coordinate system. (a) Europe. (b) Middle East.

value of the length that provides the required phase shift is estimated. This is done independently for T_x and T_y. Finally, using a zero-finding routine (Newton-Raphson method in this case), the exact value of T_x and T_y for both polarizations is found, taking into account the little coupling between the two polarizations that there may exist. Following this approach, T_x and T_y are found for each reflectarray element, and given the relations in (5), all dipole dimensions are obtained.

This design process is usually done either by employing a commercially available full-wave simulation software, which is very time-consuming, or in-house full-wave analysis tools [17], which are substantially faster but more limited in scope. However, the design process involves hundreds or even thousands of calls to this tool, and may take several hours to complete a design for a large reflectarray [6]. Consequently, techniques to accelerate this procedure without compromising accuracy are advantageous. In this work, we use SVM surrogate models to achieve this acceleration.

B. Antenna Specifications

The reflectarray for DBS application is rectangular and comprised of 74×70 unit cells in a regular grid, with a total of 5180 elements. The working frequency is 11.85 GHz and the periodicity is $14\,\text{mm} \times 14\,\text{mm}$. The feed is modeled as a $\cos^q\theta$ function, with $q = 23$, producing an illumination taper of $-18.5\,\text{dB}$ at the edges. The feed is placed at $(-0.358,\ 0,\ 1.070)\,\text{m}$ with regard to the center of the reflectarray. For this arrangement, the highest value of the angle of incidence is $\theta_{\max} = 43°$, which guarantees that no grating lobes will appear for the employed periodicity. The unit cell is the same described in Section II-A and shown in Fig. 1. In addition, one SVM is trained per angle of incidence and they are discretized as shown in Fig. 4, obtaining a total of 152 (θ, φ) pairs, which are further reduced to 76 pairs using symmetries. Thus, a total number of 190 000 are required to train all the SVMs. In contrast, the database used in [16] employs 1 980 000 samples per frequency.

The antenna is assumed placed in a satellite in geostationary orbit. Two different coverages are considered for the example, one for each linear polarization. They are shown in Fig. 5 and correspond to Europe and the Middle East. In both cases, the outer contour takes into account typical pointing errors (0.1° in roll, 0.1° in pitch and 0.5° in yaw).

C. Results

The design procedure has been applied to the reflectarray described in Section III-B with both MoM-LP and the SVM. To that end, first a Phase-Only Synthesis (POS) [24] was carried out to obtain the phase-shifts that provide the European coverage in polarization X and the Middle East coverage in polarization Y. The designs have been carried out with a laptop computer with an Intel Core i7-4712MQ CPU at 2.30 GHz. Using MoM-LP, the design took 4655.98 seconds (1 hour and 18 minutes) while using SVM it took only 8.24 seconds to complete the process. This corresponds to an acceleration factor of 565. The same reflectarray was designed in [6] with ANNs following a similar procedure, although using a different MoM-LP, where the reported acceleration factor was 207.

After carrying out the design with the MoM-LP and SVMs, both designs are simulated with MoM-LP, to assess the differences between the two tools since the MoM-LP provides more accurate simulations using the real angles of incidence at each reflectarray element. The results for the copolar patterns are shown in Fig. 6. Although there are small discrepancies between the patterns, in both designs the copolar pattern perfectly complies with the requirement of 28 dBi of minimum gain in the coverage area. In addition, the minimum gain obtained in the coverage zone for polarization X with the MoM-LP design is 28.7 dBi while for the SVM design is 28.4 dBi. For comparison, in [6] the difference in minimum

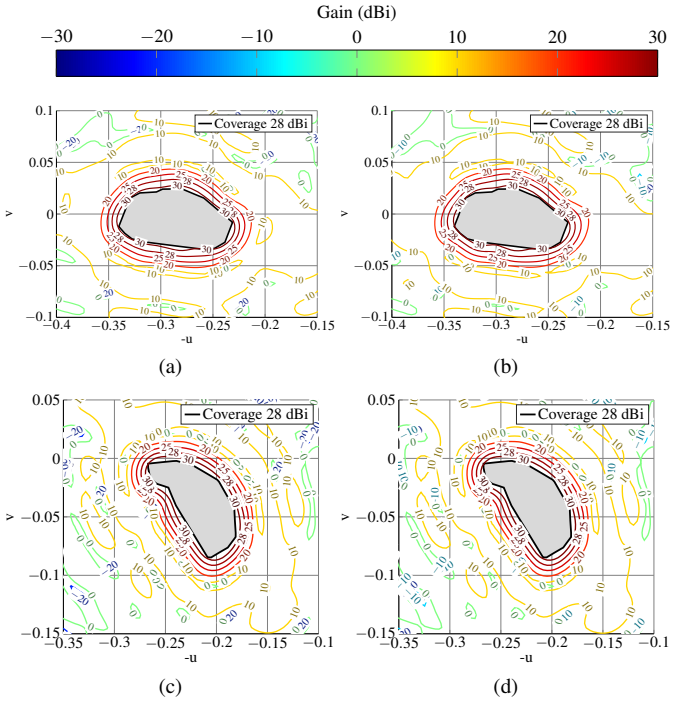

Fig. 6. Copolar radiation patterns simulated with MoM-LP using the real angles of incidence at each reflectarray element for the (a) MoM-LP design for polarization X, (b) SVM design for polarization X, (c) MoM-LP design for polarization Y, and (d) SVM design for polarization Y.

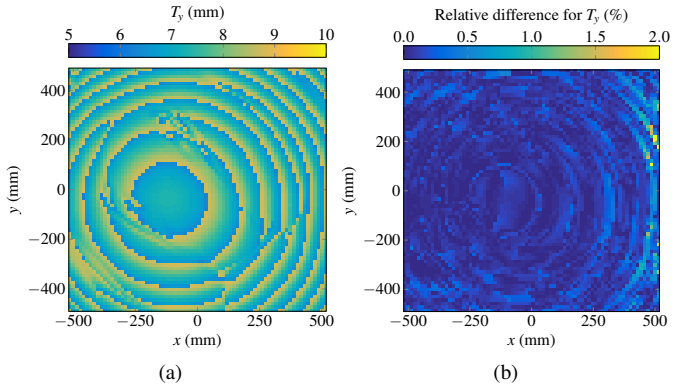

Fig. 7. For the SVM design: (a) obtained values of T_y geometrical variables; (b) relative difference of T_y with regard to the MoM-LP design using the real angles of incidence.

gain between the MoM-LP and ANN simulations is 1 dB, which is attributed to small errors in the predicted phase-shifts by the ANN. For Y polarization the minimum copolar gain in the Middle East coverage is 28.6 dBi in both cases.

Finally, Fig. 7 shows the value of T_y obtained for the design with SVM and the relative difference between the SVM and MoM-LP designs. The differences are very small even though the MoM-LP took into account the real angles of incidence and the SVM used the discretization shown in Fig. 4.

IV. Crosspolar Optimization with SVMs

A. Optimization Algorithm

For the crosspolar optimization, the generalized Intersection Approach (IA) presented in [14] is used, employing the Levenberg-Marquardt Algorithm (LMA) [25] in the backward projection. A flowchart of the optimization algorithm is shown in Fig. 8, where the main building blocks of the LMA are shown. The forward projection imposes the requirements on the radiation pattern while the backward projection minimizes the distance between the current radiation pattern and the one that complies with the specifications. For the latter task, the LMA is employed, and is set to perform three iterations per iteration of the IA, since the backward projection only requires to decrease a distance, not to reach a local minimum [26]. The optimization algorithm is independent of the polarization. In this work, dual-linear polarization is considered since the employed unit cell was conceived for dual-linear operation. However, if the reflectarray was analysed in circular polarization, using an adequate unit cell and feed, the algorithm could optimize the right and left handed components of the far field for cross-polarization improvement.

In order to effectively reduce the crosspolar component, its corresponding specification template is set to 40 dB below the maximum copolar gain and the crosspolar residual is scaled by a factor of 10^3 in linear scale. The value of 40 dB is set arbitrarily as a target with the aim of minimizing the crosspolar pattern (parameters such as the crosspolar discrimination or crosspolar isolation, discussed below, are thus improved indirectly). In addition, the optimization will be carried out in a subset of the whole visible region, corresponding to $u \in (0.05, 0.45)$ and $v \in (-0.20, 0.15)$ with a resolution of 11 187 points in a regular U-V grid. The optimization will consider two variables per reflectarray element, since the SVM has been trained with two geometrical variables (T_x and T_y). Thus, the total number of optimizing variables will be 10 360.

Two different crosspolar optimizations will be carried out using the same reflectarray presented in Section III-B. The first optimization will be that of the design with the European coverage for X polarization and the Middle East coverage for Y polarization. The goal of the optimization is to lower the crosspolar far field while preserving the copolar pattern within requirements. The second crosspolar optimization corresponds to a reflectarray with the Middle East coverage in dual-linear polarization. In contrast to the first example, this case operates in a smaller angular region imposing copolar and crosspolar conditions in the same region in both linear polarizations. For both examples, a minimum requirement of 28 dBi in the coverage zone for the copolar pattern is imposed.

Finally, the crosspolar optimization is carried out in a workstation with two Intel Xeon E5-2650v3 at 2.3 GHz.

B. Europe-Middle East Optimization

The starting point for the crosspolar optimization corresponds to the SVM design carried out in Section III-C and whose radiation pattern is shown in Fig. 6. The copolar pattern after the crosspolar optimization is shown in Fig. 9, for the MoM-LP and SVM optimizations. In both cases, the final layout was simulated with MoM-LP. Only the copolar pattern for X polarization (European coverage) is shown, since it represents the worse case. The copolar pattern is slightly affected after the optimization, but in both cases it still

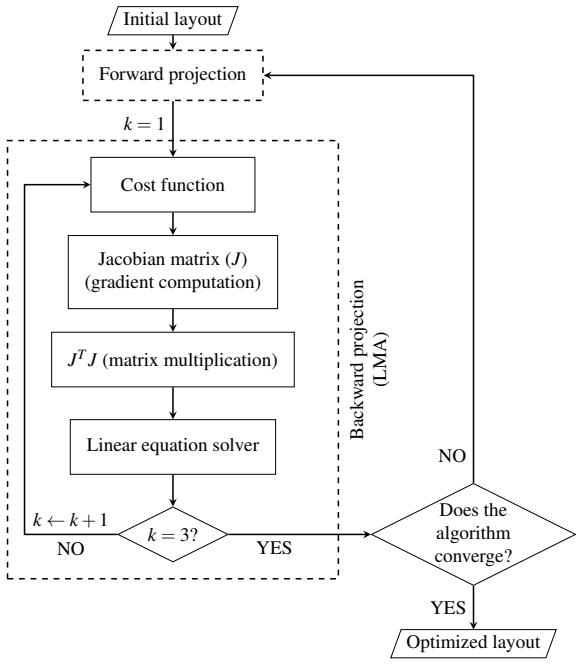

Fig. 8. Flowchart of the generalized Intersection Approach used for the crosspolar optimization of large reflectarrays for DBS applications.

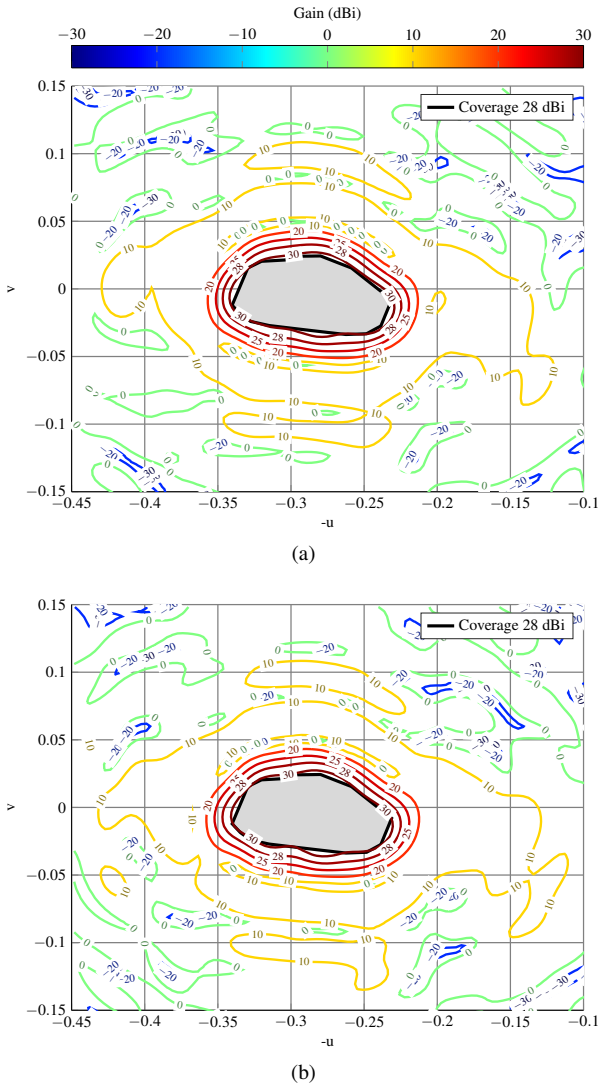

Fig. 9. Copolar pattern for X polarization with European coverage simulated with MoM-LP (taking into account the real angles of incidence at each reflectarray element) after the crosspolar optimization with (a) MoM-LP and (b) SVM.

complies with the requirement of 28 dBi in the coverage area. In fact, for the MoM-LP optimization the minimum copolar gain in the coverage area is 28.5 dBi while for the SVM optimization (and then simulated with MoM-LP) is 28.3 dBi. The starting point had a minimum copolar gain of 28.4 dBi.

Fig. 10 shows the initial and optimized crosspolar discrimination (XPD) for the coverage zone. The XPD (measured in dB) is defined as the difference, point by point, of the copolar gain and the crosspolar gain (both measured in dBi). The minimum XPD improved 5.5 dB for the optimization carried out with the SVM. Another parameter of interest is the crosspolar isolation (XPI; measured in dB), which is defined for the coverage zone as the difference between the minimum copolar gain and the maximum crosspolar gain. The initial value of the XPI was 27.57 dB, while for the MoM-LP optimization is 34.35 dB and for the SVM optimization is 32.32 dB. The drop in XPI when the SVM optimization is simulated with MoM-LP is due to small discrepancies in the minimum copolar gain and maximum crosspolar gain obtained with each technique. As demonstrated in [12], the discretization of the angles of incidence (see Fig. 4) affects the crosspolar pattern more than the copolar pattern. Nevertheless, the improvement over the initial value is 4.75 dB using the SVM for the optimization. In addition, previous works [21], [27], [28] show that, for large reflectarrays for DBS applications, the crosspolar pattern is close to fulfil requirements or they are fulfilled by little margin. Any further improvement in the crosspolar pattern, such as the ones obtained with this optimization, would allow for manufacturing tolerances and non-idealities of the working environment since the fulfilment margin would increase. Moreover, system level parameters such as the signal-to-interference-plus-noise ratio (SINR) would also improve due to the better cross-polarization performance achieved by the optimization.

Finally, Table I summarizes the main results for this optimization in both polarizations. It also includes the results from the SVM optimization when it is simulated with SVM instead of MoM-LP (fourth row), and another optimization carried out with MoM-LP using the same discretization of the angles of incidence as the SVM (third row). It is interesting to note how similar are the results obtained after the optimization with MoM-LP and SVM when the same angles of incidence are employed (third and fifth rows). Similarly, the results shown in the second and fourth rows, corresponding to the reference optimization with MoM-LP and the SVM optimization simulated with SVM are also very similar. This proves that the main source of discrepancies is the discretization of the angles of incidence and, to a lesser extent, the inaccuracies of the SVM model. In any case, the improvement over the starting point is patent in all optimizations, as shown in Table I.

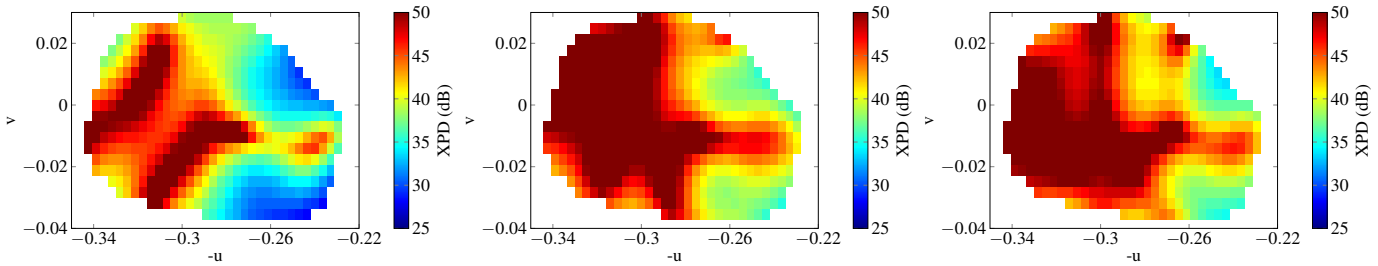

(a) (b) (c)

Fig. 10. Crosspolar discrimination (XPD) for X polarization simulated with MoM-LP for the European coverage. (a) Initial XPD ($\mathrm{XPD_{min}} = 27.78\,\mathrm{dB}$), (b) optimized with MoM-LP ($\mathrm{XPD_{min}} = 35.10\,\mathrm{dB}$) and (c) optimized with SVM ($\mathrm{XPD_{min}} = 33.26\,\mathrm{dB}$).

Table I
SUMMARY OF THE MAIN PARAMETERS FOR THE CROSSPOLAR OPTIMIZATION OF THE REFLECTARRAY WITH EUROPEAN (POLARIZATION X) AND MIDDLE EAST (POLARIZATION Y) COVERAGES. $\mathrm{CP_{min}}$ IS IN DBI; $\mathrm{XPD_{min}}$ AND XPI IN DB.

Optimization tool	Angles of incidence in optimization	Final simulation tool	Angles of incidence in final simulation	X polarization			Y polarization		
				$\mathrm{CP_{min}}$	$\mathrm{XPD_{min}}$	XPI	$\mathrm{CP_{min}}$	$\mathrm{XPD_{min}}$	XPI
None (initial layout)	—	MoM-LP	Real	28.41	27.78	27.57	28.64	28.07	26.90
MoM-LP	Real	MoM-LP	Real	28.52	35.10	34.35	28.56	36.41	34.50
MoM-LP	Discretized	MoM-LP	Real	28.32	33.23	32.37	28.66	35.06	32.99
SVM	Discretized	SVM	Discretized	28.51	35.42	34.23	28.58	35.70	34.13
SVM	Discretized	MoM-LP	Real	28.28	33.26	32.32	28.58	34.49	32.48

C. Optimization of Middle East in Dual-Linear Polarization

The second crosspolar optimization example corresponds to the same reflectarray but with the Middle East coverage in both linear polarizations. As starting point, a new design was carried out using the same phase-shift for both polarizations and following the procedure described in Section III-A. After the optimization with MoM-LP and SVM the worst results were obtained for X polarization. Again, it complies with the specifications, having a minimum copolar gain in the coverage zone of 28.76 dB for the optimization with MoM-LP and 28.44 dB for the optimization with SVM. Table II summarizes the main results for this optimization in both polarizations, obtaining the same conclusions as in the previous example.

V. DISCUSSION ON THE ACHIEVED SPEED-UP

The main goal of using the SVM to analyze reflectarray antennas is the substantial acceleration in computing the matrix of reflection coefficients while still obtaining high accuracy. However, there is an initial one-time cost accounting for the 760 SVM trainings (76 angles and 10 coefficients per angle), that for the case at hand took less than an hour using a workstation with two Intel Xeon E5-2650v3 at 2.3GHz; this is the case since the training of one SVM is independent from the rest and can be easily parallelized. In any case, using the same computer employed for the design in Section III-C and the same reflectarray comprised of 5 180 elements, the analysis with SVM takes a mean time of 34.8 ms to analyze all the elements, while using MoM-LP in the same conditions takes a mean time of 116.70 s, corresponding to a speed-up factor of 3350. This acceleration factor corresponds exclusively to a single analysis of the reflectarray. Since the design involves some operations that are not accelerated by the SVM, the acceleration factor is smaller: 565. Nevertheless, this acceleration is still close to three orders of magnitude and it means a considerable time saving on the design compared to MoM-LP.

On the other hand, the acceleration factor for the crosspolar optimization is considerably reduced since there are many operations that are not accelerated by the SVM. For the example investigated here, the slowest part of the generalized IA is the backward projector that employs the LMA (see Fig. 8; computing time of the forward projector is negligible). The LMA can be divided into four main blocks: computation of the cost function, Jacobian matrix (J), matrix multiplication ($J^T J$) and linear equation solver [25]. The use of the SVM accelerates the computation of the cost function and of the Jacobian matrix, since they are the building blocks where the reflectarray elements are analyzed. On the contrary, the matrix multiplication and linear equation solver only depend on the size of the problem which is, in this case, the number of optimizing variables and points in the U-V grid where the far field is computed.

Table III summarizes the computing time for each building block of the LMA using MoM-LP and SVM for the large reflectarray for DBS applications. While the matrix multiplication and linear equation solver computing time remain the same, the cost function and Jacobian are accelerated. However, the acceleration factor of the Jacobian computation is much smaller than the one of the cost function computation. This is caused due to the fact that the computation of the Jacobian matrix requires many more operations that are not sped up by the SVM. In particular, each column of the Jacobian only

Table II
SUMMARY OF THE MAIN PARAMETERS FOR THE CROSSPOLAR OPTIMIZATION OF THE REFLECTARRAY WITH MIDDLE EAST COVERAGE IN DUAL-LINEAR POLARIZATION. CP_{min} IS IN DBI; XPD_{min} AND XPI IN DB.

Optimization tool	Angles of incidence in optimization	Final simulation tool	Angles of incidence in final simulation	X polarization			Y polarization		
				CP_{min}	XPD_{min}	XPI	CP_{min}	XPD_{min}	XPI
None (initial layout)	—	MoM-LP	Real	28.25	31.11	29.28	28.62	31.02	29.69
MoM-LP	Real	MoM-LP	Real	28.76	36.18	34.94	28.97	36.06	34.82
MoM-LP	Discretized	MoM-LP	Real	28.47	34.79	33.15	28.93	34.66	33.36
SVM	Discretized	SVM	Discretized	28.83	36.25	34.98	28.93	36.36	34.50
SVM	Discretized	MoM-LP	Real	28.44	34.80	33.19	28.93	34.59	33.40

Table III
COMPUTING TIME IN SECONDS OF THE MAIN LMA BUILDING BLOCKS FOR THE CROSSPOLAR OPTIMIZATION OF A REFLECTARRAY COMPRISED OF 5 180 ELEMENTS AND USING A WORKSTATION WITH 40 THREADS.

Tool	FFT grid	Cost function	Jacobian	J^TJ	Solver
MoM-LP	512×512	29.49	75.08	18.94	1.28
SVM	512×512	0.13	25.53	19.47	1.29
MoM-LP	128×128	29.96	61.03	1.39	1.24
SVM	128×128	0.12	2.76	1.36	1.24

Table IV
COMPUTING TIME IN SECONDS OF THE MAIN LMA BUILDING BLOCKS FOR THE CROSSPOLAR OPTIMIZATION OF A REFLECTARRAY COMPRISED OF 900 ELEMENTS AND USING A LAPTOP WITH 8 THREADS.

Tool	FFT grid	Cost function	Jacobian	J^TJ	Solver
MoM-LP	512×512	21.53	101.99	28.62	0.03
SVM	512×512	0.23	80.37	29.08	0.02
MoM-LP	128×128	21.83	45.77	1.84	0.03
SVM	128×128	0.05	2.40	1.74	0.03

analyzes one reflectarray element using MoM-LP or SVM, while it has to compute the spectrum functions using eight FFTs. When a high resolution of 512×512 points for the FFT is employed, the acceleration factor in the computation of the Jacobian is small due to the relatively slow computations of the FFT with regard to the analysis of a single element. This does not apply to the cost function, where all the elements are analyzed and the radiation pattern is computed only once.

For the sake of comparison, the computing time was also measured with a lower resolution of 128×128 for the FFT. In this case, the contribution of the computing time of the FFTs is much smaller and thus the acceleration factor when using SVM instead of MoM-LP considerable increases (from an acceleration of roughly 3 to 22). Accordingly, the time cost of the matrix multiplication also decreases since the size of the Jacobian matrix is considerably reduced. The same pattern appears in Table IV, where the smaller reflectarray taken from [29] was optimized using the laptop described in Section III-C. In this last example, the optimization was performed in the whole visible region, instead of in a subset of the U-V grid, which accounts for the different (and lower) acceleration in the Jacobian matrix calculation for high resolutions of the FFT.

Regarding the total computing time for the crosspolar optimizations presented in Section IV, the optimization for the reflectarray with European coverage for polarization X and the Middle East coverage for polarization Y took 111 iterations of the generalized IA to achieve those results. Since three iterations of the LMA were performed for each IA iteration, this gives a total of 333 iterations where the cost function and Jacobian matrix were computed. Using MoM-LP it took approximately 11 hours and 30 minutes, while using SVM this time was reduced to 4 hours and 18 minutes. Thus, more than seven hours were saved by using SVM in this optimization. For the other example with the Middle East coverage in dual-linear polarization, the algorithm only took 24 iterations of the generalized IA, and a total of 72 iterations of the LMA. The total time using MoM-LP was two hours and a half, while using the SVM it was 56 minutes, thus saving more than 90 minutes. Please note that in all these cases the employed FFT resolution was 512×512 points.

From the results shown in Tables III and IV it is clear that the use of SVMs to accelerate crosspolar optimization is not enough. The computation of the gradient (Jacobian matrix) in local search algorithms is also highly dependent on the FFT resolution, which is related to the number of points in which the far field is computed. For small- or medium-sized reflectarrays lower resolutions may be used along with SVMs to accelerate more than one order of magnitude the optimizations. However, this might not be possible for larger reflectarrays. Since larger antennas are more directive, higher resolution is required, especially for stringent applications such as DBS, where a good resolution in the coverage zone is necessary. Thus, alternatives to a lower resolution to accelerate the computation of the Jacobian matrix are required.

One approach could be the use of multiresolution UV grids using the Non-Uniform FFT (NUFFT) [30]. In this case, although the NUFFT is slower than the FFT [31], the employed U-V grid would have high resolution in the area of interest while few points are used elsewhere to account for the side lobes. In this way, the employed grid would have far fewer points than the typical high-resolution grid of the FFT, and computations would be accelerated for the Jacobian matrix and the matrix multiplication. Another approach, compatible

with the use of a multiresolution grid, is to avoid the use of the (NU)FFT in the computation of the Jacobian. This is possible by taking only into account the differential contribution of the array element which is modified to compute the far field. Progress is being made in this regard to further accelerate the computation of the Jacobian matrix as well as the matrix multiplication.

Finally, the achieved acceleration in this work, plus the potential further acceleration mentioned above, paves the way towards the optimization of even larger reflectarrays that are being proposed for applications such as Synthetic Radar Aperture (SAR) [32] or multibeam coverage [33]. These reflectarrays are comprised of tens of thousands of elements, and thus, the optimization process would be extremely slow without accelerating techniques, since the computational time increases with the cube of the number of optimizing variables due to the matrix multiplication, while the time for filling the Jacobian matrix grows quadratically. In addition, since a local-search algorithm is employed, several runs of the optimization algorithm employing different starting points and/or tuning different parameters such as a weighting function may be necessary in order to avoid undesired local minima. This is especially true for applications with very stringent requirements, such as [21], where there are multiple coverage zones, each one with different requirements, and fine-tuning of different weighting constants in the cost function is most likely necessary to comply with both copolar and crosspolar specifications.

VI. Conclusions

In this work, machine learning techniques in the form of Support Vector Machines (SVMs) have been used for the first time for the design and crosspolar optimization of reflectarray antennas. The goal was to obtain a surrogate model of the reflectarray unit cell to use in substitution of a full-wave analysis technique based on local periodicity. The use of this surrogate model speeds up the analysis of the whole antenna more than three orders of magnitude. The design process of a dual-polarized reflectarray antenna is detailed to accurately find the element geometry that matches the required phase-shift for two linear polarizations. Then, a large reflectarray for Direct Broadcast Satellite (DBS) application is designed with MoM-LP and SVM following this procedure. An acceleration factor close to three orders of magnitude is obtained for the design when using SVM instead of MoM-LP while still obtaining accurate results. Finally, SVMs were applied to accelerate the crosspolar optimization of the same large reflectarray for space communications. Two examples are provided, one with a different coverage footprint for each linear polarization (Europe and the Middle East) and another example with the same coverage footprint working in dual-linear polarization (Middle East). In both cases the XPD and XPI are greatly improved while computations are accelerated thanks to the use of SVMs instead of MoM-LP. However, the acceleration factor for the crosspolar optimization is considerably dependent on the resolution of the far field and in some cases the use of the SVM gives acceleration factors lower than one order of magnitude. Nevertheless, further computational improvements are currently under research to accelerate the computation of the gradient.

References

[1] D. Caputo, A. Pirisi, M. Mussetta, A. Freni, P. Pirinoli, and R. E. Zich, "Neural network characterization of microstrip patches for reflectarray optimization," in *3rd European Conference on Antennas and Propagation (EuCAP)*, Berlin, Germany, Mar. 23–27, 2009, pp. 2520–2522.

[2] M. Musseta, P. Pirinoli, P. T. Cong, M. Orefice, and R. E. Zich, "Characterization of microstrip reflectarray square ring elements by means of an Artificial Neural Network," in *Proceedings of the Fourth European Conference on Antennas and Propagation (EuCAP)*, Barcelona, Spain, Apr. 12–16, 2010, pp. 1–4.

[3] S. Nesil, F. Güneş, and U. Özkaya, "Phase characterization of a reflectarray unit cell with minkowski shape radiating element using multilayer perceptron neural network," in *7th International Conference on Electrical and Electronics Engineering (ELECO)*, vol. 2, Bursa, Turkey, Dec. 1–4, 2011, pp. 219–222.

[4] H. M. Linh, M. Mussetta, P. Pirinoli, and R. E. Zich, "Modeling of reflectarray elements by means of metaPSO-based artificial neural network," in *7th European Conference on Antennas and Propagation (EuCAP)*, Gothenburg, Sweden, Apr. 8–12, 2013, pp. 3450–3451.

[5] P. Robustillo, J. Zapata, J. A. Encinar, and J. Rubio, "ANN characterization of multi-layer reflectarray elements for contoured-beam space antennas in the Ku-band," *IEEE Trans. Antennas Propag.*, vol. 60, no. 7, pp. 3205–3214, Jul. 2012.

[6] P. Robustillo, J. Zapata, J. A. Encinar, and M. Arrebola, "Design of a contoured-beam reflectarray for a eutelsat european coverage using a stacked-patch element characterized by an artificial neural network," *IEEE Antennas Wireless Propag. Lett.*, vol. 11, pp. 977–980, 2012.

[7] A. Freni, M. Mussetta, and P. Pirinoli, "Neural network characterization of reflectarray antennas," *Int. J. Antennas Propag.*, vol. 2012, pp. 1–10, May 2012.

[8] V. Richard, R. Loison, R. Gillard, H. Legay, and M. Romier, "Loss analysis of a reflectarray cell using ANNs with accurate magnitude prediction," in *11th European Conference on Antennas and Propagation (EuCAP)*, Paris, France, Mar. 19–24, 2017, pp. 2402–2405.

[9] P. Robustillo, J. Zapata, J. A. Encinar, R. Florencio, R. R. Boix, and J. R. Mosig, "Accurate characterization of multi-resonant reflectarray cells by artificial neural networks," in *The 8th European Conference on Antennas and Propagation (EUCAP)*, The Hague, The Netherlands, Apr. 6–11, 2014, pp. 2297–2299.

[10] F. Güneş, S. Nesil, and S. Demirel, "Design and analysis of Minkowski reflectarray antenna using 3-D CST Microwave Studio-based neural network model with particle swarm optimization," *Int. J. RF Microw. Comput. Eng.*, vol. 23, no. 2, pp. 272–284, Mar. 2013.

[11] L. Tenuti, G. Oliveri, D. Bresciani, and A. Massa, "Advanced learning-based approaches for reflectarrays design," in *11th European Conference on Antennas and Propagation (EuCAP)*, Paris, France, Mar. 19–24, 2017, pp. 84–87.

[12] D. R. Prado, J. A. López-Fernández, G. Barquero, M. Arrebola, and F. Las-Heras, "Fast and accurate modeling of dual-polarized reflectarray unit cells using support vector machines," *IEEE Trans. Antennas Propag.*, vol. 66, no. 3, pp. 1258–1270, Mar. 2018.

[13] C. Wan and J. A. Encinar, "Efficient computation of generalized scattering matrix for analyzing multilayered periodic structures," *IEEE Trans. Antennas Propag.*, vol. 43, no. 11, pp. 1233–1242, Nov. 1995.

[14] D. R. Prado, M. Arrebola, M. R. Pino, R. Florencio, R. R. Boix, J. A. Encinar, and F. Las-Heras, "Efficient crosspolar optimization of shaped-beam dual-polarized reflectarrays using full-wave analysis for the antenna element characterization," *IEEE Trans. Antennas Propag.*, vol. 65, no. 2, pp. 623–635, Feb. 2017.

[15] M. Zhou, S. B. Sørensen, O. S. Kim, E. Jørgensen, P. Meincke, and O. Breinbjerg, "Direct optimization of printed reflectarrays for contoured beam satellite antenna applications," *IEEE Trans. Antennas Propag.*, vol. 61, no. 4, pp. 1995–2004, Apr. 2013.

[16] M. Zhou, S. B. Sørensen, O. S. Kim, E. Jørgensen, P. Meincke, O. Breinbjerg, and G. Toso, "The generalized direct optimization technique for printed reflectarrays," *IEEE Trans. Antennas Propag.*, vol. 62, no. 4, pp. 1690–1700, Apr. 2014.

[17] J. Huang and J. A. Encinar, *Reflectarray Antennas*. Hoboken, NJ, USA: John Wiley & Sons, 2008.

[18] D. R. Prado, M. Arrebola, M. R. Pino, and F. Las-Heras, "Complex reflection coefficient synthesis applied to dual-polarized reflectarrays with cross-polar requirements," *IEEE Trans. Antennas Propag.*, vol. 63, no. 9, pp. 3897–3907, Sep. 2015.
[19] B. Schölkopf and A. J. Smola, *Learning with Kernels*, 1st ed. Cambridge, Massachusetts: The MIT Press, 2001.
[20] R. Florencio, R. R. Boix, and J. A. Encinar, "Enhanced MoM analysis of the scattering by periodic strip gratings in multilayered substrates," *IEEE Trans. Antennas Propag.*, vol. 61, no. 10, pp. 5088–5099, Oct. 2013.
[21] J. A. Encinar, R. Florencio, M. Arrebola, M. A. Salas-Natera, M. Barba, J. E. Page, R. R. Boix, and G. Toso, "Dual-polarization reflectarray in Ku-band based on two layers of dipole arrays for a transmit-receive satellite antenna with South American coverage," *Int. J. Microw. Wirel. Technol.*, vol. 10, no. 2, pp. 149–159, 2018.
[22] M. Salucci, L. Tenuti, G. Oliveri, and A. Massa, "Efficient prediction of the EM response of reflectarray antenna elements by an advanced statistical learning method," *IEEE Trans. Antennas Propag.*, vol. 66, no. 8, pp. 3995–4007, Aug. 2018.
[23] R. Florencio, J. A. Encinar, R. R. Boix, V. Losada, and G. Toso, "Reflectarray antennas for dual polarization and broadband telecom satellite applications," *IEEE Trans. Antennas Propag.*, vol. 63, no. 4, pp. 1234–1246, Apr. 2015.
[24] D. R. Prado, M. Arrebola, M. R. Pino, and F. Las-Heras, "Improved reflectarray phase-only synthesis using the generalized intersection approach with dielectric frame and first principle of equivalence," *Int. J. Antennas Propag.*, vol. 2017, pp. 1–11, May 2017.
[25] D. R. Prado, J. Álvarez, M. Arrebola, M. R. Pino, R. G. Ayestarán, and F. Las-Heras, "Efficient, accurate and scalable reflectarray phase-only synthesis based on the Levenberg-Marquardt algorithm," *Appl. Comp. Electro. Society Journal*, vol. 30, no. 12, pp. 1246–1255, Dec. 2015.
[26] O. M. Bucci, G. D'Elia, G. Mazzarella, and G. Panariello, "Antenna pattern synthesis: a new general approach," *Proc. IEEE*, vol. 82, no. 3, pp. 358–371, Mar. 1994.
[27] J. A. Encinar, L. S. Datashvili, J. A. Zornoza, M. Arrebola, M. Sierra-Castaner, J. L. Besada-Sanmartin, H. Baier, and H. Legay, "Dual-polarization dual-coverage reflectarray for space applications," *IEEE Trans. Antennas Propag.*, vol. 54, no. 10, pp. 2827–2837, Oct. 2006.
[28] J. A. Encinar, M. Arrebola, L. F. de la Fuente, and G. Toso, "A transmit-receive reflectarray antenna for direct broadcast satellite applications," *IEEE Trans. Antennas Propag.*, vol. 59, no. 9, pp. 3255–3264, Sep. 2011.
[29] D. R. Prado, M. Arrebola, M. R. Pino, F. Las-Heras, R. Florencio, R. R. Boix, and J. A. Encinar, "Reflectarray antenna with reduced crosspolar radiation pattern," in *10th European Conference on Antennas and Propagation (EuCAP)*, Davos, Switzerland, Apr. 10–15, 2016, pp. 1–5.
[30] D. R. Prado, M. Arrebola, M. R. Pino, F. Las-Heras, and J. A. Encinar, "Efficient computation of the reflectarray far fields in adaptive grids for speed improvement," in *IEEE International Symposium on Antennas and Propagation (APSURSI)*, San Diego, California, USA, Jul. 9–14, 2017, pp. 1181–1182.
[31] D. R. Prado, M. Arrebola, M. R. Pino, and F. Las-Heras, "An efficient calculation of the far field radiated by non-uniformly sampled planar fields complying Nyquist theorem," *IEEE Trans. Antennas Propag.*, vol. 63, no. 2, pp. 862–865, Feb. 2015.
[32] C. Tienda, M. Younis, P. López-Dekker, and P. Laskowski, "Ka-band reflectarray antenna system for SAR applications," in *The 8th European Conference on Antennas and Propagation (EUCAP)*, The Hague, The Netherlands, Apr. 6–11, 2014, pp. 1603–1606.
[33] E. Martínez-de-Rioja, J. A. Encinar, A. Pino, B. González-Valdés, S. V. Hum, and C. Tienda, "Bifocal design procedure for dual reflectarray antennas in offset configurations," *IEEE Antennas Wireless Propag. Lett.*, vol. 17, no. 8, pp. 1421–1425, Aug. 2018.

Daniel R. Prado was born in Sama de Langreo, Asturias, Spain, in 1986. He received the B.Sc., M.Sc., and Ph.D. degrees in telecommunication engineering from the University of Oviedo, Gijón, Spain, in 2011, 2012, and 2016, respectively.

From 2010 to 2011, he was with The Institute of Electronics, Communications and Information Technology, Queen's University Belfast, Belfast, U.K., where he was involved in the design of leaky-wave antennas as part of his B.Sc. research project. From 2011 to 2017, he was a Research Assistant with the Signal Theory and Communications Area, University of Oviedo, where he was involved in the development of efficient techniques for the analysis and synthesis of reflectarray antennas. In 2014, he was with the School of Electrical Engineering, KTH Royal Institute of Technology, Stockholm, Sweden, as a Visiting Scholar, where he was involved in transformation optics applied to dielectric lenses. Since 2018, he has been with the Institute of Sensors, Signals and Systems, Heriot-Watt University, Edinburgh, U.K. His current research interests include the analysis of nonuniform arrays and the development of efficient techniques for the analysis and optimization of near and far fields of reflectarray antennas.

Dr. Prado was a recipient of a Predoctoral Scholarship financed by the Gobierno del Principado de Asturias and a Postdoctoral Fellowship partially financed by the European Union.

Jesús A. López-Fernández was born in Avilés, Asturias, Spain. He received the M.Sc. and the Ph.D. degrees in telecommunication engineering from the University of Vigo, Spain, in 1999 and 2009, respectively.

From April 2002 to March 2003, he was a Marie-Curie Visiting Fellow at the Mechanical & Manufacturing Engineering Department, Trinity College Dublin (TCD). Since October 2003, he has been with the Electrical Engineering Department, University of Oviedo, Asturias, Spain, where he is currently an Associate Professor teaching courses on Digital Communications and Radar Systems. His research interests include iterative methods and speed-up schemes applied to scattering problems, parallel algorithms, and signal processing techniques.

Manuel Arrebola (S'99–M'07–SM'17) was born in Lucena (Córdoba), Spain. He received the M.Sc. degree in telecommunication engineering from the University of Málaga, Málaga, Spain, in 2002, and the Ph.D. degree from the Technical University of Madrid (UPM), Madrid, Spain, in 2008.

From 2003 to 2007, he was with the Electromagnetism and Circuit Theory Department, UPM, as a Research Assistant. In 2005, he was with the Microwave Techniques Department, Universität Ulm, Ulm, Germany, as a Visiting Scholar. In 2007, he joined the Electrical Engineering Department, Universidad de Oviedo, Gijón, Spain, where he is currently an Associate Professor. In 2009, he enjoyed a two-month stay at the European Space Research and Technology Centre, European Space Agency, Noordwijk, The Netherlands. In 2018, he was a Visiting Professor with the Edward S. Rogers Sr. Department of Electrical & Computer Engineering, University of Toronto, Toronto, Canada. His current research interests include the development of efficient analysis, design and optimization techniques of reflectarray and transmitarray antennas both in near and far field.

Dr. Arrebola was a co-recipient of the 2007 S. A. Schelkunoff Transactions Prize Paper Award given by the IEEE Antennas and Propagation Society.

George Goussetis (S'99–M'02–SM'12) received the Diploma degree in electrical and computer engineering from the National Technical University of Athens, Athens, Greece, in 1998 and the Ph.D. degree from the University of Westminster, London, UK, in 2002. In 2002 he also graduated B.Sc. in physics (first class) from University College London (UCL), London, U.K.

In 1998, he joined Space Engineering, Rome, Italy, as an RF Engineer. In 1999, he joined the Wireless Communications Research Group, University of Westminster, as a Research Assistant. Between 2002 and 2006, he was a Senior Research Fellow at Loughborough University, Loughborough, U.K. He was a Lecturer (Assistant Professor) with Heriot-Watt University, Edinburgh, U.K., between 2006 and 2009, and a Reader (Associate Professor) with Queen's University Belfast, U.K., between 2009 and 2013. In 2013, he joined Heriot-Watt University as a Reader and was promoted to Professor in 2014, where he currently directs the Institute of Sensors, Sigals and Systems. He has authored or co-authored over 500 peer-reviewed papers, five book chapters, and one book. He holds four patents. His current research interests include microwave and antenna components and subsystems.

Dr. Goussetis was a recipient of a Research Fellowship from the Onassis Foundation in 2001, the U.K. Royal Academy of Engineering from 2006 to 2011, and the European Marie-Curie Experienced Researcher Fellowships from 2011 to 2012 and from 2014 to 2017. He was a co-recipient of the 2011 European Space Agency Young Engineer of the Year Prize, the 2011 EuCAP Best Student Paper Prize, the 2012 EuCAP Best Antenna Theory Paper Prize, and the 2016 Bell Labs Prize. He has served as an Associate Editor for the IEEE ANTENNAS AND WIRELESS PROPAGATION LETTERS.